

Cloning, characterization, and engineering of fungal L-arabinitol dehydrogenases

Byoungjin Kim · Ryan P. Sullivan · Huimin Zhao

Received: 3 January 2010 / Revised: 26 March 2010 / Accepted: 29 March 2010 / Published online: 23 April 2010
© Springer-Verlag 2010

Abstract L-Arabinitol 4-dehydrogenase (LAD) catalyzes the conversion of L-arabinitol to L-xylulose with concomitant NAD⁺ reduction in fungal L-arabinose catabolism. It is an important enzyme in the development of recombinant organisms that convert L-arabinose to fuels and chemicals. Here, we report the cloning, characterization, and engineering of four fungal LADs from *Penicillium chrysogenum*, *Pichia guilliermondii*, *Aspergillus niger*, and *Trichoderma longibrachiatum*, respectively. The LAD from *P. guilliermondii* was inactive, while the other three LADs were NAD⁺-dependent and showed high catalytic activities, with *P. chrysogenum* LAD being the most active. *T. longibrachiatum* LAD was the most thermally stable and showed the maximum activity in the temperature range of 55–65°C with the other LADs showed the maximum activity in the temperature range of 40–50°C. These LADs were active from pH 7 to 11 with an optimal pH of 9.4. Site-directed

mutagenesis was used to alter the cofactor specificity of these LADs. In a *T. longibrachiatum* LAD mutant, the cofactor preference toward NADP⁺ was increased by 2.5 × 10⁴-fold, whereas the cofactor preference toward NADP⁺ of the *P. chrysogenum* and *A. niger* LAD mutants was also drastically improved, albeit at the expense of significantly reduced catalytic efficiencies. The wild-type LADs and their mutants with altered cofactor specificity could be used to investigate the functionality of the fungal L-arabinose pathways in the development of recombinant organisms for efficient microbial L-arabinose utilization.

Keywords Arabinose fermentation · Xylitol production · Alcohol dehydrogenase · Cofactor specificity · Ethanol production

Electronic supplementary material The online version of this article (doi:10.1007/s00253-010-2593-4) contains supplementary material, which is available to authorized users.

B. Kim · R. P. Sullivan · H. Zhao
Energy Biosciences Institute,
University of Illinois at Urbana-Champaign,
Urbana, IL 61801, USA

R. P. Sullivan · H. Zhao
Department of Chemical and Biomolecular Engineering,
University of Illinois at Urbana-Champaign,
Urbana, IL 61801, USA

H. Zhao (✉)
Department of Chemistry, Biochemistry and Bioengineering,
Institute for Genomic Biology,
University of Illinois at Urbana-Champaign,
Urbana, IL 61801, USA
e-mail: zhao5@illinois.edu

Introduction

L-Arabinose is a major constituent of lignocellulosic biomass (Lee 1997; Chandrakant and Bisaria 1998), and its efficient utilization is essential for economical conversion of lignocellulosic biomass to value-added products such as bioethanol and xylitol. *Saccharomyces cerevisiae* is a suitable organism for bioethanol production (Almeida and Hahn-Hägerdal 2009; Matsushika et al. 2009a; Matsushika et al. 2009b). However, native *S. cerevisiae* is unable to metabolize L-arabinose, and recombinant *S. cerevisiae* strains harboring a fungal L-arabinose utilization pathway have shown limited success (Richard et al. 2003b; Bettiga et al. 2009).

One of the major limitations results from the poor performance of the L-arabinitol 4-dehydrogenase (LAD) in the fungal L-arabinose utilization pathway. LAD is a Zn²⁺-containing alcohol dehydrogenase (Richard et al. 2001;

Sullivan and Zhao 2007). In the fungal L-arabinose catabolic pathway, L-arabinose is reduced to L-arabinitol by an aldose reductase, which is subsequently oxidized to L-xylulose by LAD. L-Xylulose reductase reduces L-xylulose to xylitol, which is introduced to the pentose phosphate pathway after further oxidation and phosphorylation (Richard et al. 2003a). Accumulation of L-arabinitol has been observed in recombinant *S. cerevisiae* strains, which suggests an inefficient conversion of L-arabinitol to L-xylulose by the LAD (McMillan and Boynton 1994; Verho et al. 2004; Matsushika et al. 2008). Analogous to L-arabinitol accumulation, xylitol accumulates during D-xylose consumption by recombinant yeast strains, and it has been suggested that this is due to the different cofactor preferences of the enzymes in the initial D-xylose utilization pathway (Eliasson et al. 2001; Jeppsson et al. 2005). Recombinant *S. cerevisiae* strains containing the xylose reductase and xylitol dehydrogenase with altered cofactor specificities have demonstrated improved D-xylose utilization and reduced xylitol formation during ethanolic fermentation (Bengtsson et al. 2009; Matsushika et al. 2009b). Therefore, it is highly desirable to identify an LAD enzyme that exhibits high catalytic efficiency in *S. cerevisiae* and cofactor preference consistent with other enzymes in the L-arabinose utilization pathway.

Here, we report the cloning and characterization of four fungal LADs from *Penicillium chrysogenum*, *Pichia guilliermondii*, *Aspergillus niger*, and *Trichoderma longibrachiatum* (*Trichoderma reesei*). The last two enzymes were reported in the literature; however, their enzymatic properties have not been characterized in detail (Richard et al. 2001; Pail et al. 2004; de Groot et al. 2005). In addition, we report the successful alteration of cofactor preference of these LADs from NAD⁺ to NADP⁺ by site-directed mutagenesis.

Materials and methods

Materials All gene and protein sequences used in this study were obtained from the National Center for Biotechnology Information (www.ncbi.nlm.nih.gov). *A. niger* (NRRL 326), *P. guilliermondii* (NRRL Y2075), and *P. chrysogenum* (NRRL 807) were obtained from the United States Department of Agriculture Agricultural Research Service Culture Collection (Peoria, IL). *T. longibrachiatum* (*T. reesei*, YSM 768) was obtained from the German Resource Centre for Biological Material (DSMZ). *E. coli* DH5 α , BL21(DE3), and pET-28a were purchased from Novagen (Madison, WI). Transcriptor First Strand cDNA synthesis kit, isopropyl- β -D-thiogalactopyranoside (IPTG), NADH, NADPH, NAD⁺, and NADP⁺ were purchased from Roche (Mannheim, Germany). Wizard[®] Genomic DNA purification kit was purchased from Promega (Madison, WI). Phusion polymerase and restriction

enzymes *Nde*I, *Eco*RI, and *Bam*HI and buffers for their reactions were purchased from New England Biolabs (Beverly, MA). L-Arabinitol was obtained from MP Bio-medicals (Solon, OH). Kanamycin, lysozyme, and bovine serum albumin were purchased from Sigma-Aldrich (St. Louis, MO). The QIAprep spin plasmid mini-prep kit, QIAquick PCR purification kit, QIAquick gel purification kit, and RNeasy miniprep kit were purchased from Qiagen (Valencia, CA). Oligonucleotide primers were obtained from Integrated DNA Technologies (Coralville, IA). Co²⁺ Talon[™] immobilized metal affinity resin was purchased from Clontech BD Biosciences (San Jose, CA). Amicon[®] Ultra-15 filtration devices (molecular cutoff 10,000 Da) were purchased from Millipore (Billerica, MA). Reagents for protein assay, sodium dodecylsulfate–polyacrylamide gel electrophoresis (SDS–PAGE), protein size marker, protein molecular weight standard, and size-exclusion column (Bio-Sil SEC-250, 300 \times 7.8 mm) were purchased from Bio-Rad (Hercules, CA). All other chemicals were purchased from Thermo-Fisher Scientific (Pittsburgh, PA) unless otherwise specified.

DNA cloning *A. niger*, *T. longibrachiatum*, *P. chrysogenum*, and *P. guilliermondii* were grown in liquid media or on agar plates containing 1% yeast extract, 2% peptone, and 2% L-arabinose. Cells were frozen in liquid nitrogen for the isolation of total RNA or genomic DNA. Reverse transcription–polymerase chain reaction (RT–PCR) was performed on mRNAs isolated from *T. longibrachiatum*, *P. chrysogenum*, and *P. guilliermondii* to obtain cDNA, and PCR was used to obtain the genes encoding (putative) LADs. For *A. niger*, the putative LAD gene could not be amplified from cDNA due to some unknown reasons. Thus, overlap extension–PCR (OE–PCR) was used to clone this intron-containing gene from the isolated genomic DNA. Note that all primer sequences used to clone these genes are listed in Table S1 in [Electronic supplementary materials](#). PCR products were subcloned into pET-28a vector, and the constructs were used to transform into two *E. coli* strains, DH5 α and BL21 (DE3), by electroporation for cloning and expression, respectively. *Nde*I/*Bam*HI restriction sites were used for the subcloning of the predicted genes from *A. niger*, *T. longibrachiatum*, and *P. guilliermondii*, and *Nde*I/*Eco*RI sites were used for *P. chrysogenum*. The constructs encoded (putative) LADs as an N-terminal His₆-tagged fusion. Plasmids were sequenced using BigDye[®] Terminator sequencing method and analyzed with 3730xL Genetic Analyzer (Applied Biosystems, Foster City, CA) at the Biotechnology Center at the University of Illinois at Urbana-Champaign (Urbana, IL). The proteins encoded by these four genes from *A. niger*, *T. longibrachiatum*, *P. chrysogenum*, and *P. guilliermondii* are referred to as anLAD, tLAD, pLAD, and pGLAD, respectively, hereafter.

Protein expression and purification *E. coli* BL21 (DE3) containing the LAD genes was grown overnight at 30°C on a rotary shaker at 250 rpm. Overnight culture (50 µL) was used to inoculate a fresh culture (5 mL), which was grown at 30°C with shaking at 250 rpm until the optical density at 600 nm (OD₆₀₀) reached 0.6–1.0. The cultures were then induced with 0.3 mM IPTG at 30°C for 3–4 h or at 18°C for 20 h.

The induced cells (1 mL) were lysed by resuspending in 1 mL of 50 mM potassium phosphate buffer (pH 7.0) with 1 mg/mL lysozyme and shaken at 30°C and 250 rpm for 30 min. Cells were kept at –80°C overnight and thawed at room temperature. The resulting cell lysates were centrifuged at 13,200 rpm for 15 min, and the supernatant and precipitate were analyzed for protein expression by SDS–PAGE. Ten microliters of cell lysate was used for an activity assay with 200 mM L-arabinitol and 2 mM NAD⁺ as the substrates in 50 mM potassium phosphate buffer (pH 7.0). NADH production was monitored by measuring absorbance at 340 nm ($\epsilon=6.22 \text{ mM}^{-1} \text{ cm}^{-1}$) using a Cary 300 Bio UV–vis spectrophotometer (Varian, Cary, NC).

For protein purification, the induced cells (400 mL) were treated with 15 mL of Buffer A (20 mM Tris, 0.5 M NaCl, 20% glycerol, pH 7.6) with 1 mg/mL lysozyme and shaken at 30°C and 250 rpm for 30 min. After a freeze-thaw cycle, the resulting product was further lysed by sonication followed by centrifugation for 20 min at 12,000 rpm to remove cell debris. The supernatants were applied to a column packed with Co²⁺-immobilized metal affinity chromatography resin to purify His₆-tagged proteins following the manufacturer's instructions. The purified proteins were desalted by ultrafiltration (Amicon Ultra, Millipore) and washed with HEPES buffer (pH 7.0) containing 150 mM NaCl and 15% glycerol and kept at –20°C. Protein concentrations were determined by the Bradford method (Bradford 1976) according to the manufacturer's protocol.

Steady-state kinetics Initial rates were determined by measuring the absorbance change at 340 nm using a UV–vis spectrophotometer at room temperature in 50 mM potassium phosphate buffer (pH 7.0). Initial rates were measured at various concentrations of the substrate (L-arabinitol) and cofactors (NAD⁺/NADP⁺) (5 to 320 mM for L-arabinitol, 0.5 to 3.2 mM for cofactors). Enzyme kinetics for the substrate and cofactors were analyzed using Michaelis–Menten kinetics, and kinetic parameters were determined by fitting data to the Lineweaver–Burk plot. The parameters for substrate were determined by measuring initial rates at saturated cofactor concentrations (3.2 mM), and those for cofactors were determined at saturated substrate concentrations (320 mM). Assays were performed in triplicate.

Molecular weight and quaternary structure The molecular weights of the proteins were determined using a Bio-Sil SEC-250 column (300×7.8 mm, Bio-Rad, Hercules, CA) on a Shimadzu HPLC system (Shimadzu, Kyoto, Japan). The mobile phase consists of 50 mM Na₂HPO₄, 50 mM NaH₂PO₄, 150 mM NaCl, and 10 mM NaN₃ (pH 6.8), and the flow rate was 1.0 mL/min. The molecular weights were calculated by comparing the retention times with those of protein molecular weight standard. The quaternary structures were determined based on the molecular weights observed by HPLC and the molecular weights of monomeric subunits which were determined by SDS–PAGE analysis.

Temperature and pH dependence The optimal temperatures of the proteins were determined by assaying enzyme activities at temperatures ranging from 10°C to 70°C. Thermal inactivation was determined by measuring enzyme activity after various incubation times at 50°C in phosphate buffer. Enzyme activity was measured with 2 mM NAD⁺ and 200 mM L-arabinitol. Half-life of enzyme activity was determined using a first-order exponential decay function. Temperature was controlled by a Cary temperature controller connected to the UV–vis spectrophotometer (Varian, Cary, NC). pH-dependent enzyme activity was determined by measuring activity at pH between 5.0 and 11.0 at saturated concentrations of NAD⁺ (2 mM) and L-arabinitol (200 mM) in a universal buffer (50 mM morpholineethanesulfonic acid/50 mM Tris/50 mM glycine; Ellis and Morrison 1982).

Metal analysis Duplicate samples for metal analysis were prepared in phosphate buffered saline (PBS) by buffer exchange and lyophilization. Each sample contained 1–2 mg of protein in 1 mL buffer solution. The identity and content of the metal were analyzed by inductively coupled plasma atomic emission spectrometry (OES Optima 2000 DV, Perkin Elmer, Boston, MA) in the Microanalytical Laboratory at the University of Illinois at Urbana-Champaign (Urbana, IL).

LAD engineering for NADP⁺ Site-directed mutagenesis was performed to alter the cofactor specificity of each LAD from NAD⁺ to NADP⁺. Detailed approaches and experimental details were described elsewhere (Sullivan 2009). Briefly, the sequences of cloned LADs were aligned with the *N. crassa* LAD (ncLAD) sequence, and the corresponding amino acids to those found in NADP⁺-dependent ncLAD mutant were mutated. Two amino acid residues within the β - α - β motif of the coenzyme binding domain were replaced with serine and arginine, respectively: D213 and I214 for anLAD, D224 and I225 for tLAD, and D212 and I213 for pcLAD (Korkhin et al. 1998; Pauly et al. 2003; Watanabe et al. 2005). The third mutation was introduced at A359 for anLAD, A362 for tLAD, and S358 for pcLAD and replaced with threonine

(for primer sequences, see Table S2 in [Electronic supplementary materials](#)). Megaprimer PCR method was used to introduce site-specific mutations using wild-type LAD constructs as the templates (Sarkar and Sommer 1990). Correct mutations were confirmed by DNA sequence analysis.

Results

Putative LAD gene identification, cloning, and expression - From a protein BLAST search using nLAD (EAA36547.1) as a probe, two putative genes were identified in *P. chrysogenum* (XP_002569286.1) and *P. guilliermondii* (EDK37120.2), respectively. The amino acid sequence identities of these two proteins with nLAD were 71% and 46%, respectively. Along with these two putative LAD genes, the genes encoding anLAD (CAH69383.1) and tlLAD (AAL08944.1) were cloned into the pET-28a vector and expressed in *E. coli* BL21 (DE3). The amino acid sequence identities of anLAD and tlLAD with nLAD were 70% and 80%, respectively. All the constructs produced both soluble and insoluble His₆-tagged proteins, and their sizes were around 40 kDa (Fig. 1). Calculated molecular weights of the subunits of the four proteins were 43 kDa (anLAD), 41 kDa (tlLAD), 42 kDa (pcLAD), and 42 kDa (pgLAD). In the activity assays with cell-free extracts, an-, tl-, and pcLAD showed dehydrogenase activities with L-arabinitol. The putative gene in *P. guilliermondii* was cloned and confirmed by DNA sequencing, and its expression was checked by SDS-PAGE analysis (Fig. 1). However, no dehydrogenase activity was observed in cell-free lysate with L-arabinitol. Therefore, the hypothetical protein cloned from *P. guilliermondii* was not considered for further analysis.

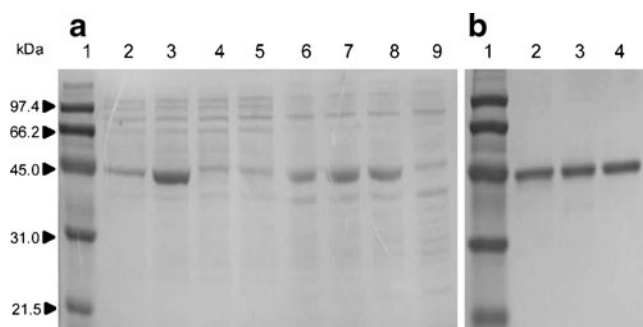


Fig. 1 Expression and purification of recombinant LADs. **a** SDS-PAGE of cell-free extracts. Lane 1 molecular weight marker, lanes 2–5 soluble fractions, lanes 6–9 insoluble fractions in cell-free lysate overexpressing LADs from *A. niger*, *T. longibrachiatum*, *P. chrysogenum*, and *P. guilliermondii*, respectively

Steady-state kinetics The cloned LADs showed different binding affinities and catalytic activities for L-arabinitol: K_m differed by twofold and k_{cat} by about threefold among the LADs. For L-arabinitol, the K_m values of anLAD, tlLAD, and pcLAD were 25 ± 1 , 18 ± 1 , and 37 ± 2 mM, and the k_{cat} values were 507 ± 22 , 346 ± 41 , and $1,085 \pm 71$ min⁻¹, respectively (Table 1). The tlLAD enzyme had the lowest K_m , while pcLAD showed the highest catalytic activity (k_{cat}) and efficiency (k_{cat}/K_m) despite having the highest K_m (Table 1). For cofactor NAD⁺ kinetics, the cloned LADs showed K_m values in the range of 0.2–0.3 mM and catalytic efficiencies in the range of 2,526 to 3,460 mM⁻¹·min⁻¹ (Table 2). All cloned LADs showed minimal activities toward NADP⁺ (Tables 1 and 2). The initial rates were not saturated at highest substrate and cofactor concentration (320 mM for L-arabinitol and 3.2 mM for NADP⁺) due to the large K_m . Therefore, only the catalytic efficiency of the enzyme was determined using 0.1 or 0.2 mM for NADP⁺ and 10 or 20 mM for L-arabinitol ($K_m \gg [S]$; Tables 1 and 2).

Temperature and pH dependence The optimal temperatures of anLAD and pcLAD were between 40°C and 50°C, while tlLAD showed higher optimal temperature between 55°C and 65°C (Fig. 2a). Catalytic activities of the LADs exponentially decreased with the length of incubation time at 50°C and were almost completely deactivated after 100 min (Fig. 2b). tlLAD was the most thermally stable with a half-life of 20 min at 50°C, and anLAD was least stable with a half-life of less than 5 min at 50°C. All LADs characterized showed activity in the pH range of 7 to 11 with a maximum activity around pH 9.4 (Fig. 2c). In the pH range outside of 9 to 10, activity was significantly reduced, and approximately 20% of activity remained at pH 7.0 (Fig. 2c). No activity was detected at or below pH 5.0 (data not shown).

Table 1 Kinetic parameters of LADs for L-arabinitol at saturated cofactor concentrations

		Specific activity (U/mg protein)	K_m (mM)	k_{cat} (min ⁻¹)	k_{cat}/K_m (mM ⁻¹ ·min ⁻¹)
anLAD	NAD ⁺	11.7±0.3 ^a	25±1	507±22	20.0±0.8
	NADP ⁺	– ^b	–	–	0.04±0.01
tlLAD	NAD ⁺	8.7±0.1	18±1	346±41	19.0±0.8
	NADP ⁺	–	–	–	0.13±0.02
pcLAD	NAD ⁺	25.3±1.4	37±2	1,085±71	29±1
	NADP ⁺	–	–	–	0.04±0.02

^a Error indicates standard error of the mean, $n=3$

^b Dash indicates not determined due to high K_m for indicated cofactor

Table 2 Kinetic parameters of LADs for NAD⁺ and NADP⁺ at saturated L-arabinitol concentration

		K_m (mM)	k_{cat} (min ⁻¹)	k_{cat}/K_m (mM ⁻¹ ·min ⁻¹)
anLAD	NAD ⁺	0.20±0.01 ^a	494±11	2,526±83
	NADP ⁺	– ^b	–	20±9
tlLAD	NAD ⁺	0.2±0.1	436±96	2,689±646
	NADP ⁺	–	–	17±9
pcLAD	NAD ⁺	0.3±0.1	1,039±165	3,460±505
	NADP ⁺	–	–	15±4

^a Error indicates standard error of the mean, $n=3$

^b Dash indicates not determined due to high K_m for indicated cofactor

Metal analysis and quaternary structure Molecular weights of an-, tl-, and pcLAD were determined to be 178, 194, and 173 kDa, respectively. Comparing to the molecular weights of the subunits determined by SDS-PAGE, results suggest that the LADs are noncovalently linked tetramers in their native forms. Measured weight percentages of Zn²⁺ were close to those calculated based on the 1:1 molar ratio (Table S3 in [Electronic supplementary materials](#)).

LAD engineering for altered cofactor specificity The tlLAD mutant showed significantly altered cofactor specificity from NAD⁺ to NADP⁺ and also the highest catalytic activity. The K_m and k_{cat} of the tlLAD mutant for L-arabinitol with NADP⁺ were 46±4 mM and 170±9 min⁻¹, respectively (Table 3). In all assays including the tlLAD mutant with saturated NAD⁺, a plateau of reaction rate was not observed in the tested concentration range, so catalytic efficiencies were determined at 0.8 mM for NAD⁺ and 80 mM for L-arabinitol (Tables 3 and 4). For cofactors, anLAD and tlLAD mutants showed significantly higher preference for NADP⁺ over NAD⁺ (Table 4). The K_m values of the anLAD and tlLAD mutants were 0.46±0.09 and 0.10±0.01 mM, and the k_{cat} values were 55.7±6.4 and 90.5±9.2 min⁻¹, respectively (Table 4). The catalytic efficiencies of anLAD and tlLAD mutants were 130±32 and 934±72 mM⁻¹·min⁻¹, and the ratios of the catalytic efficiencies with NADP⁺ to NAD⁺ were 100 and 161, respectively. For the tlLAD mutant, the ratio of catalytic efficiency for NADP⁺ to NAD⁺ was increased by 2.5×10⁴-fold (Tables 2 and 4). The pcLAD mutant showed no activity with NAD⁺.

Discussion

Largely driven by the need to isolate new LADs for the development of recombinant organisms that convert L-arabinose to fuels and chemicals, we sought to clone, characterize, and engineer four LAD genes from fungi. All

four cloned putative LADs contain regions conserved in Zn-dependent alcohol dehydrogenases and Rossmann-fold NAD(P)⁺-binding proteins. The hypothetical protein from *P. chrysogenum* had 71% sequence identity with nLAD and was found to encode a highly active LAD. Although

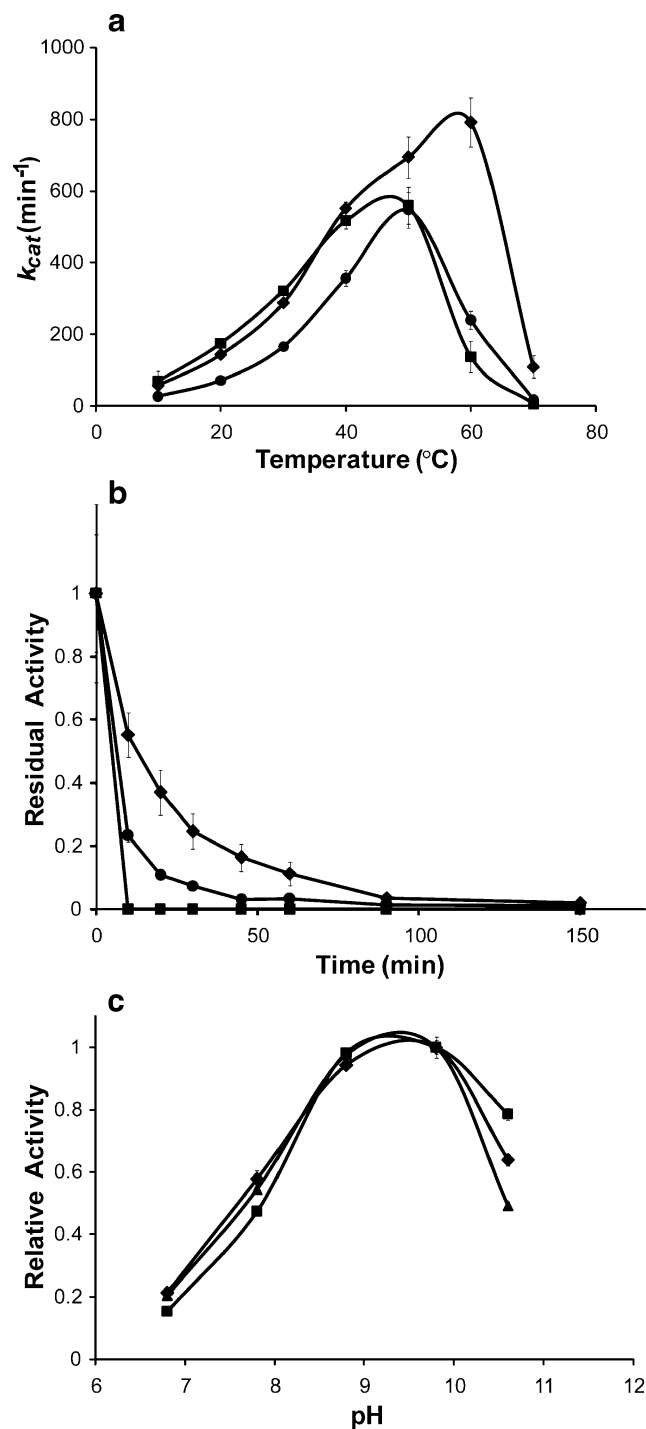


Fig. 2 Thermal and pH-dependent properties of the LADs: *A. niger* (filled square), *T. longibrachiatum* (filled diamond), *P. chrysogenum* (filled circle). **a** Temperature-dependent catalytic activities. **b** Thermal inactivation at 50°C over time. **c** pH-dependent catalytic activities. Error bars indicate standard error of the mean ($n=3$)

Table 3 Kinetic parameters of LAD mutants for L-arabinitol at saturated cofactor concentrations

		Specific activity (U/mg protein)	K_m (mM)	k_{cat} (min ⁻¹)	k_{cat}/K_m (mM ⁻¹ ·min ⁻¹)
anLAD mutant	NAD ⁺	– ^a	–	–	0.010±0.002 ^b
	NADP ⁺	–	–	–	0.45±0.20
tlLAD mutant	NAD ⁺	–	–	–	0.050±0.007
	NADP ⁺	3.9±0.2	46±4	170±9	3.7±0.2
pcLAD mutant	NAD ⁺	–	–	–	–
	NADP ⁺	–	–	–	0.02±0.02

^a Dash indicates not determined due to high K_m for indicated cofactor

^b Error indicates standard error of the mean, $n=3$

the protein from *P. guilliermondii* contained the same conserved regions, it had only 46% sequence identity with ncLAD and was not active for L-arabinitol with either NAD⁺ or NADP⁺. This suggests that the hypothetical protein from *P. guilliermondii* is not an LAD and might take other polyols or arabinose isomers as a substrate.

Among the characterized LADs, pcLAD was the most active enzyme for both substrate and cofactors, and its turnover number (k_{cat}) was more than twofold higher than that of the other LADs. tlLAD showed the highest binding affinity for L-arabinitol (lowest K_m), compensating for its low catalytic activity (Table 1). Although all characterized LADs showed detectable activities for L-arabinitol with NADP⁺, these wild-type LADs would preferentially utilize NAD⁺ as cofactor in vivo due to the large K_m with NADP⁺ (0.2–0.3 mM for NAD⁺ and >1.6 mM for NADP⁺).

There are a few studies reporting the kinetic parameters of LADs, and these values are largely dependent on the experimental conditions including pH, buffer, and substrate concentrations. Previously reported ncLAD had higher catalytic activity ($k_{cat}=1,206$ min⁻¹) and efficiency (67 mM⁻¹·min⁻¹) than the LADs characterized in this study; however, it should be noted that those values were determined at pH 8.0, and the purification tag was cleaved off (Sullivan and Zhao 2007). Taking the more than twofold difference in the catalytic activity between pH 7.0 and 8.0 (Fig. 1c) into account, the kinetic properties of these LADs would be comparable with those of ncLAD. Specific activity of tlLAD (previously *Hypocrea jecorina*) was reported to be between 0.013 and 1.6 U/mg (Richard et al. 2001; Pail et al. 2004). These values were obtained with partially purified protein or a subsaturated cofactor concentration (0.25 mM) with purified enzyme. K_m of tlLAD was measured to be 18±1 mM for L-arabinitol and 0.2±0.01 mM for NAD⁺, and these values were consistent with the literature data of 4.5–40 mM for L-arabinitol and 0.18 mM for NAD⁺ (Richard et al. 2001; Pail et al. 2004). The specific activity of anLAD was 11.8±0.3 U/mg protein and reported to be 96 U/mg at pH 9.6 with partially

purified protein (de Groot et al. 2005). However, $K_{m,L-arabinitol}$ of 89 mM was also significantly higher than the value determined in this study (25±1 mM), resulting in low catalytic efficiency (k_{cat}/K_m) (de Groot et al. 2005).

The characterized LADs shared the tetrameric structure with ncLAD, and with homologous enzymes D-sorbitol and xylitol dehydrogenase (Korkhin et al. 1998; Pauly et al. 2003). ncLAD was reported to contain close to two Zn²⁺ ions per subunit (Sullivan and Zhao 2007). One zinc ion is involved in catalytic function (Nordling et al. 2002; Riveros-Rosas et al. 2003), and the other structural zinc is thought to be involved in enzyme stability (Banfield et al. 2001; Watanabe et al. 2005). Although all characterized LADs contained the amino acid sequence for structural Zn²⁺ binding (CNACEPCLTGRYNGC, Fig. S1 in Electronic supplementary materials), metal analysis data suggested that a subunit possesses one Zn²⁺, possibly in the active site. Similarly, it was reported that D-sorbitol dehydrogenase from *Bacillus subtilis* contained one Zn²⁺ per subunit despite the presence of the conserved sequence for structural Zn²⁺ binding (Ng et al. 1992). The cloned LADs had a much shorter half-life at 50°C compared with ncLAD, and this

Table 4 Kinetic parameters of LAD mutants for NAD⁺ and NADP⁺ at saturated L-arabinitol concentration

		K_m (mM)	k_{cat} (min ⁻¹)	k_{cat}/K_m (mM ⁻¹ ·min ⁻¹)
anLAD mutant	NAD ⁺	– ^a	–	1.3±0.3 ^b
	NADP ⁺	0.46±0.09	55.7±6.4	130±32
tlLAD mutant	NAD ⁺	–	–	5.8±0.8
	NADP ⁺	0.097±0.011	90.5±9.2	934±72
pcLAD mutant	NAD ⁺	–	–	–
	NADP ⁺	–	–	3.6±1.0

^a Dash indicates not determined due to high K_m for indicated cofactor

^b Error indicates standard error of the mean, $n=3$

relatively lower thermal stability might be due to the absence of structural Zn²⁺.

The protein engineering for altering cofactor specificity was most successful with tLAD, which has the highest sequence identity with nLAD (80%). The K_m of the tLAD mutant for NADP⁺ was even lower than the K_m of the wild-type tLAD for NAD⁺. However, the K_m for L-arabinitol was increased from 18 to 46 mM, and the catalytic activity was reduced to approximately 50% of the wild-type tLAD. The other LAD mutants also showed altered cofactor specificity toward NADP⁺ with significantly higher K_m (>160 mM for L-arabinitol and >1.6 mM for cofactor) and reduced catalytic efficiency. In nLAD engineering for reversed cofactor specificity, the mutations on D211 and I212 were selected by rational design based on the known residues responsible for cofactor specificity (Sullivan 2009). The mutation on S348 was found through directed evolution using error-prone PCR and had more significant impact on the catalytic activity rather than the cofactor binding affinity. The first two residues were conserved between the LADs, while the third one was not in the multiple alignment analysis, as it was alanine in wild-type anLAD and tLAD (Fig. S1 in [Electronic supplementary materials](#)). Mutation of all three residues enabled the cofactor specificity to be reversed for all LADs characterized, but tLAD resulted in the largest improvement. This suggests that the cofactor specificity conferring residues from nLAD are somewhat context dependent, and further analysis of these residues or continued engineering on anLAD or pLAD would be necessary to improve cofactor specificity.

In this study, we cloned and characterized three highly active LADs from *P. chrysogenum*, *A. niger*, and *T. longibrachiatum*, respectively. The characterized LADs share common biochemical properties with previously known Zn²⁺-dependent dehydrogenases but differ in enzymatic kinetics, thermal stability, and optimal temperature. We also demonstrated that cofactor preference could be altered from NAD⁺ to NADP⁺, which could alleviate imbalanced cofactor utilization in recombinant *S. cerevisiae*. Availability of LADs with well-characterized enzymatic properties could be useful for the engineering of recombinant L-arabinose catabolic pathways.

Acknowledgments This work was funded by the BP Energy Biosciences Institute.

References

- Almeida JRM, Hahn-Hägerdal B (2009) Developing *Saccharomyces cerevisiae* strains for second generation bioethanol: improving xylose fermentation and inhibitor tolerance. *Int Sugar J* 111:172–180
- Banfield MJ, Salvucci ME, Baker EN, Smith CA (2001) Crystal structure of the NADP(H)-dependent ketose reductase from *Bemisia argentifolii* at 2.3 angstrom resolution. *J Mol Biol* 306:239–250
- Bengtsson O, Hahn-Hägerdal B, Gorwa-Grauslund MF (2009) Xylose reductase from *Pichia stipitis* with altered coenzyme preference improves ethanolic xylose fermentation by recombinant *Saccharomyces cerevisiae*. *Biotechnol Biofuels* 2
- Bettiga M, Bengtsson O, Hahn-Hägerdal B, Gorwa-Grauslund MF (2009) Arabinose and xylose fermentation by recombinant *Saccharomyces cerevisiae* expressing a fungal pentose utilization pathway. *Microb Cell Fact* 8:40
- Bradford MM (1976) A rapid and sensitive method for the quantitation of microgram quantities of protein utilizing the principle of protein-dye binding. *Anal Biochem* 72:248–254
- Chandrakant P, Bisaria VS (1998) Simultaneous bioconversion of cellulose and hemicellulose to ethanol. *Crit Rev Biotechnol* 18:295–331
- de Groot MJL, Prathumpai W, Visser J, Ruijter GJG (2005) Metabolic control analysis of *Aspergillus niger* L-arabinose catabolism. *Biotechnol Prog* 21:1610–1616
- Eliasson A, Hofmeyr JS, Pedler S, Hahn-Hägerdal B (2001) The xylose reductase/xylitol dehydrogenase/xylulokinase ratio affects product formation in recombinant xylose-utilising *Saccharomyces cerevisiae*. *Enzyme Microb Technol* 29:288–297
- Ellis KJ, Morrison JF (1982) Buffers of constant ionic strength for studying pH-dependent processes. *Methods Enzymol* 87:405–426
- Jeppsson M, Bengtsson O, Franke K, Lee H, Hahn-Hägerdal B, Gorwa-Grauslund MF (2005) The expression of a *Pichia stipitis* xylose reductase mutant with higher K_m for NADPH increases ethanol production from xylose in recombinant *Saccharomyces cerevisiae*. *Biotechnol Bioeng* 93:665–673
- Korkhin Y, Kalb AJ, Peretz M, Bogin O, Burstein Y, Frolov F (1998) NADP-dependent bacterial alcohol dehydrogenases: crystal structure, cofactor-binding and cofactor specificity of the ADHs of *Clostridium beijerinckii* and *Thermoanaerobacter brockii*. *J Mol Biol* 278:967–981
- Lee J (1997) Biological conversion of lignocellulosic biomass to ethanol. *J Biotechnol* 56:1–24
- Matsushika A, Watanabe S, Kodaki T, Makino K, Inoue H, Murakami K, Takimura O, Sawayama S (2008) Expression of protein engineered NADP⁺-dependent xylitol dehydrogenase increases ethanol production from xylose in recombinant *Saccharomyces cerevisiae*. *Appl Microbiol Biotechnol* 81:243–255
- Matsushika A, Inoue H, Murakami K, Takimura O, Sawayama S (2009a) Bioethanol production performance of five recombinant strains of laboratory and industrial xylose-fermenting *Saccharomyces cerevisiae*. *Bioresour Technol* 100:2392–2398
- Matsushika A, Inoue H, Watanabe S, Kodaki T, Makino K, Sawayama S (2009b) Efficient bioethanol production by a recombinant flocculent *Saccharomyces cerevisiae* strain with a genome-integrated NADP(+)-dependent xylitol dehydrogenase gene. *Appl Environ Microbiol* 75:3818–3822
- Mcmillan JD, Boynton BL (1994) Arabinose utilization by xylose-fermenting yeasts and fungi. *Appl Biochem Biotechnol* 45:569–584
- Ng K, Ye RQ, Wu XC, Wong SL (1992) Sorbitol dehydrogenase from *Bacillus subtilis*—purification, characterization, and gene cloning. *J Biol Chem* 267:24989–24994
- Nordling E, Jornvall H, Persson B (2002) Medium-chain dehydrogenases/reductases (MDR). Family characterizations including genome comparisons and active site modelling. *Eur J Biochem* 269:4267–4276
- Pail M, Peterbauer T, Seiboth B, Hametner C, Druzhinina I, Kubicek CP (2004) The metabolic role and evolution of L-arabinitol 4-dehydrogenase of *Hypocrea jecorina*. *Eur J Biochem* 271:1864–1872

- Pauly TA, Ekstrom JL, Beebe DA, Chrnyk B, Cunningham D, Griffor M, Kamath A, Lee SE, Madura R, Mcguire D, Subashi T, Wasilko D, Wafts P, Mylari BL, Oates PJ, Adams PD, Rath VL (2003) X-ray crystallographic and kinetic studies of human sorbitol dehydrogenase. *Structure* 11:1071–1085
- Richard P, Londesborough J, Putkonen M, Kalkkinen N, Penttila M (2001) Cloning and expression of a fungal L-arabinitol 4-dehydrogenase gene. *J Biol Chem* 276:40631–40637
- Richard P, Verho R, Putkonen M, Londesborough J, Penttila M (2003a) The fungal L-arabinose catabolic pathway. *Yeast* 20: S218–S218
- Richard P, Verho R, Putkonen M, Londesborough J, Penttila M (2003b) Production of ethanol from L-arabinose by *Saccharomyces cerevisiae* containing a fungal L-arabinose pathway. *FEMS Yeast Res* 3:185–189
- Riveros-Rosas H, Julian-Sanchez A, Villalobos-Molina R, Pardo JP, Pina E (2003) Diversity, taxonomy and evolution of medium-chain dehydrogenase/reductase superfamily. *Eur J Biochem* 270:3309–3334
- Sarkar G, Sommer SS (1990) The megaprimer method of site-directed mutagenesis. *Biotechniques* 8:404–407
- Sullivan RP (2009) Engineering a fungal L-arabinose pathway toward the co-utilization of hemicellulosic sugars for production of xylitol. Ph. D. Dissertation University of Illinois, Urbana
- Sullivan R, Zhao HM (2007) Cloning, characterization, and mutational analysis of a highly active and stable L-arabinitol 4-dehydrogenase from *Neurospora crassa*. *Appl Microbiol Biotechnol* 77:845–852
- Verho R, Putkonen M, Londesborough J, Penttila M, Richard P (2004) A novel NADH-linked L-xylulose reductase in the L-arabinose catabolic pathway of yeast. *J Biol Chem* 279:14746–14751
- Watanabe S, Kodaki T, Makino K (2005) Complete reversal of coenzyme specificity of xylitol dehydrogenase and increase of thermostability by the introduction of structural zinc. *J Biol Chem* 280:10340–10349